

File ID 351435
Filename 5: Outlook for ecologists

SOURCE (OR PART OF THE FOLLOWING SOURCE):

Type Dissertation
Title Rise and fall of periodic patterns in a generalized Klausmeier-Gray-Scott model
Author S. van der Stelt
Faculty Faculty of Science
Year 2012
Pages v, 128
ISBN 978-90-6464-527-3

FULL BIBLIOGRAPHIC DETAILS:

<http://dare.uva.nl/record/407130>

Copyright

It is not permitted to download or to forward/distribute the text or part of it without the consent of the author(s) and/or copyright holder(s), other than for strictly personal, individual use.

Chapter 5

Outlook for ecologists

In ecology, we are interested in many features of semi-arid ecosystems, not the least among which are pattern formation from a homogeneously vegetated state and early-warning signs for desertification [41, 46, 74, 91]. For example, for the GKGS-model (0.5) we have derived parameter combinations for which the homogeneously vegetated state (U_+, V_+) destabilizes and a patterned state appears. Since the Ginzburg-Landau equation serves to describe the patterns if the precipitation rate is slightly below threshold, we can perfectly describe the appearance of patterns in the GKGS-model (0.5). On the other hand, in this thesis we did not at all consider the determination of early warning signs captured by the GKGS-model.

More generally, despite recent field studies that revealed a power-law in the patch-size distribution of the vegetation [45] that were successful in explaining the distribution by the use of cellular automata, profound insight in ecological signs of imminent desertification is basically lacking. Moreover, although reaction-diffusion(-advection) models are used extensively to model semi-arid ecosystems, early warning mechanisms have neither been consistently described nor studied by these models.

This chapter aims at describing the relevant ecological consequences of the results of this thesis, as well as at a description of possible future work. It will be argued that the Busse balloons that have been constructed in chapter 3 will be of vital importance in further analyses of desertification in the GKGS-model.

5.1 Discussion of results

In original nondimensional parameters, the GKGS-model reads

$$\begin{aligned} u_t &= u_{xx} + \nu u_x + a - Lu - Muv^2 \\ v_t &= d_v v_{xx} - bv + Nuv^2 \end{aligned} \quad (1.1)$$

with $u(x, t), v(x, t) : \mathbb{R} \times \mathbb{R}_+ \rightarrow \mathbb{R}$ and $a, b, \nu \geq 0, d_v \geq 0$. Now, u can be directly interpreted as the water infiltration and w is the vegetation density. No-

tice that, following the results of chapters 2 and 3, we model the spread of water infiltration with diffusion and not with porous media flow / nonlinear diffusion. From [46] we quote estimates for the case that the vegetation consists of grass: $\nu = 365 \text{ m year}^{-1}$ (it increases from 0 m year^{-1}), $a = 250$ to $750 \text{ kg H}_2\text{O m}^{-2} \text{ year}^{-1}$, $L = 4 \text{ year}^{-1}$, $M = 100 \text{ kg H}_2\text{O m}^{-2} \text{ year}^{-1} \text{ kg dry mass m}^{-2}$, $b = 1.8 \text{ year}^{-1}$, $d_v = 1.0 \text{ m}^2 \text{ year}^{-1}$, $N = 0.3 \text{ kg dry mass m}^{-2} \text{ year}^{-1}$.

The three homogeneous background states or equilibria from system (1.1) can now be written as

$$u_{\pm} = \frac{1}{2}[a \pm \sqrt{a^2 - 4b^2}] \quad \text{and} \quad v_{\pm} = \frac{1}{2b}[a \mp \sqrt{a^2 - 4b^2}] \quad (1.2)$$

and the desert state $(u_0, v_0) = (\frac{a}{L}, 0)$. Of course, just as in the GKGS-system (0.5), the desert state (u_0, v_0) and the vegetated equilibrium (u_+, v_+) are stable with respect to homogeneous perturbations; the vegetated equilibrium (u_-, v_-) is always unstable.

Just as before, the stable periodic patterns appear at a supercritical Turing-Hopf bifurcation at $a = a_{\text{TH}}(\nu)$. Near the Turing-Hopf bifurcation at a_{TH} , they form an Eckhaus band of stable patterns. When the condition $0 < a_{\text{TH}} - a \ll 1$ breaks down, we can no longer derive a modulation equation to obtain insight in the dynamics of (1.1) and we have to resort to continuation methods. So, we have constructed two Busse balloons for (1.1), one for $\nu = 0 \text{ m year}^{-1}$ and one for $\nu = 365 \text{ m year}^{-1}$ with the further parameters drawn from [46]: $a = 250$ to $750 \text{ kg H}_2\text{O m}^{-2} \text{ year}^{-1}$, $L = 4 \text{ year}^{-1}$, $M = 100 \text{ kg H}_2\text{O m}^{-2} \text{ year}^{-1} \text{ kg dry mass m}^{-2}$, $b = 1.8 \text{ year}^{-1}$, $d_v = 1 \text{ m}^2 \text{ year}^{-1}$, $N = 0.3 \text{ kg dry mass m}^{-2} \text{ year}^{-1}$. However, we have to choose a rate for the diffusion coefficient d_u as well (Klausmeier's model does not include diffusion of water). We assume $d_v = 1000$. This way, the diffusion coefficients of both d_v and d_u differ by a factor 1000. Though it may at first sight seem as if with this choice the diffusion of water ($d_v = 1000$) outranges the advection of water ($\nu = 365$), this is not the case. To see this, we rescale d_v to $d_v = 1$. This can be done by rescaling x with $x = \sqrt{1000} \tilde{x}$, which gives rescaled parameters $\tilde{d}_v = 1$ and $\tilde{\nu} = 11.5$ and $\tilde{d}_u = 0.001$, as is the standard setting in chapter 2. Thus, advection clearly dominates diffusion. The constructed Busse balloons are shown in Figures 5.1(a) and 5.1(b) and 5.2.

5.2 Ecological interpretation of results

From Figure 5.1, one derives that $a_{\text{TH}}(0) \approx 1.05 \cdot 10^3 \text{ kg H}_2\text{O m}^{-2} \text{ year}^{-1}$ and $a_{\text{TH}}(365) \approx 1.13 \cdot 10^3 \text{ kg H}_2\text{O m}^{-2} \text{ year}^{-1}$. Therefore, we deduce that the background state (u_+, v_+) destabilizes at a (slightly) higher precipitation rate when the gradient slope of the terrain is steeper. We interpret this as follows: on terrains with a nontrivial gradient slope, the water runs downhill without infiltrating the soil. Therefore, the homogeneous vegetation state (u_+, v_+) at terrains with a nontrivial gradient slope destabilizes into a patterned state at a higher precipitation rate than homogeneous vegetation on flat terrains, where water slowly infiltrates the soil without running off.

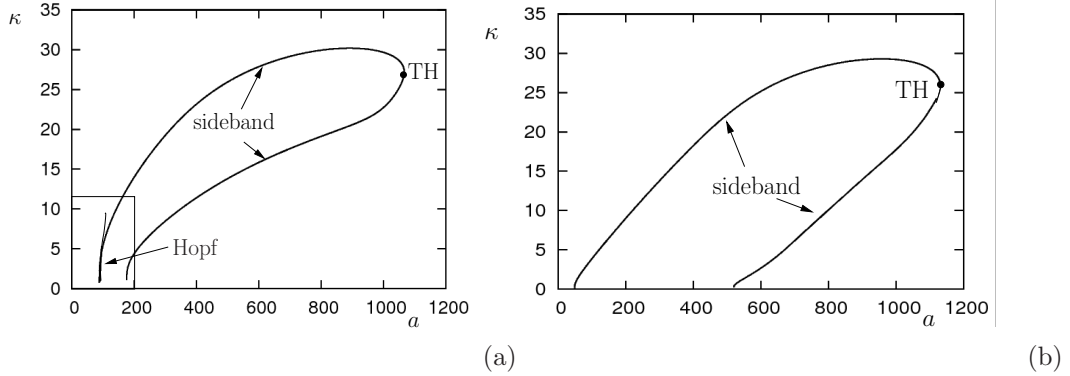


Figure 5.1: (a) Busse balloon for the GKGS-system in ecologically meaningful parameters (1.1) with $\nu = 0 \text{ m year}^{-1}$ and $b = 1.8 \text{ year}^{-1}$. An enlargement of the indicated rectangle is presented in Figure 5.2. (b) Busse balloon for the GKGS-system in ecologically meaningful parameters (1.1) with $\nu = 365 \text{ m year}^{-1}$ and $b = 1.8 \text{ year}^{-1}$. Both Busse balloons have been depicted on the same scale.

5.2.0.1 Near desertification An other striking fact observed in the Busse balloons for the GKGS-model (1.1) is that the upper branch of sideband instabilities crosses the a -axis for positive $a > 0$, both for $\nu = 0 \text{ m year}^{-1}$ and for $\nu = 365 \text{ m year}^{-1}$. Notice that this is a difference with the Busse balloons that we found for the GKGS-system in the scaling of (0.5) that have been constructed in chapter 3, where the critical value of a quickly dropped to 0 for ν increased slightly above 0 (see section 4.3.2). Numerical checks for other ν have confirmed that for each ν , there exists a precipitation rate $a = a_0^-(\nu) > 0$ such that there is no spatially periodic pattern (for any wavenumber κ).

When a is smaller than a_{TH} , the boundary of the Busse balloons in Figure 5.1 consists of sideband instabilities. For $\nu = 0 \text{ m year}^{-1}$, the upper curve of sideband instabilities is crossed by the Hopf dance that has been discussed in chapter 4. See Figure 5.1(a)¹. Therefore, spatially periodic patterns on a flat terrain destabilize into the desert state through a Hopf instability, while, at the other hand, spatially periodic patterns on a terrain with a nontrivial gradient slope destabilize into the desert state through a sideband instability. This yields one of the most intriguing ecological questions induced by our mathematical analysis: is it possible to observe from a patterned state whether it is close to a sideband instability or whether it is close to a Hopf instability?

Also, $a_0^-(\nu)$ is a decreasing function of ν : if the gradient slope increases, there are stable spatially periodic patterns for ever smaller precipitation rates. From Figure 5.1 we deduce that $a_0^-(0) \approx 8.8 \cdot 10^1 \text{ kg H}_2\text{O m}^{-2} \text{ year}^{-1}$ and $a_0^-(365) \approx$

¹In Figure 5.1(a), we have traced out an ‘approximate’ Hopf dance: the Hopf curve depicted in Figure 5.1(a) does not consist of γ -eigenvalues for fixed γ

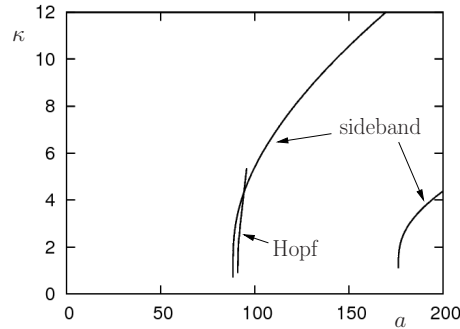


Figure 5.2: Hopf curve for the GKGS-system in ecologically meaningful parameters with $\nu = 0 \text{ m year}^{-1}$ and $b = 1.8 \text{ year}^{-1}$. Enlargement of the inset of the Busse balloon from Figure 5.1(a).

$5.0 \cdot 10^1 \text{ kg H}_2\text{O m}^{-2} \text{ year}^{-1}$. Loosely formulated, this means that desertification for systems with a nontrivial gradient slope happens at a *lower* precipitation rate than for systems that are flat. This may be understood by the following arguments. If the precipitation rate is small, then in the bare areas soil tends to dry out and becomes impermeable for water infiltration, so that precipitation that falls down in the bare areas eventually evaporates. The (scarce) vegetated areas are penetrated by roots that moisturize the soil, which entails that water from precipitation that falls down in vegetated areas infiltrates the soil. In systems with a nontrivial gradient slope, water runs downhill until it reaches a vegetated spot where it is taken up by the roots. In a flat system, water cannot run and will evaporate in the course of time, leaving only the water that falls on the vegetated areas to be taken up by plant roots. Therefore, if the precipitation rate is low, in flat systems there is more stress on vegetation growth than in systems that have nontrivial gradient slope.

Thus, we conclude that a steeper gradient considerably increases the total area of the Busse balloon: for each wavenumber κ , there is a considerable larger interval $(a_{\kappa}^-, a_{\kappa}^+)$ for which stable spatially periodic patterns exist (compare Figure 5.1(a) to 5.1(b)).

An initially stable spatially periodic pattern will for decreasing a in principle not change its wavenumber, as long as (a, κ) remains inside the Busse balloon. When an initially stable pattern gradually approaches the boundary of the Busse balloon, it will, at a further decrease of the precipitation rate a , eventually destabilize. However, at the lower precipitation rate a the specific shape of the Busse balloon depicted in Figure 5.1 generally allows for stable periodic patterns with a smaller wavenumber. See Figure 5.3. Therefore, if the decrease in a is not too fast, it is expected that the original stable spatially periodic pattern is adapted such that its wavenumber becomes smaller. Note that this mechanism of decreasing the wavenumber as a consequence

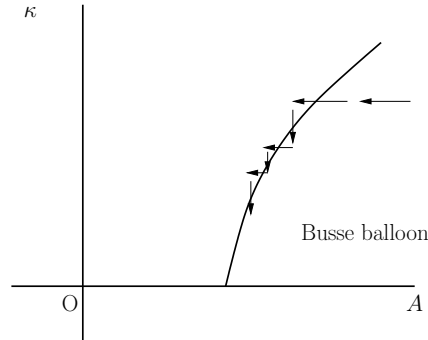


Figure 5.3: Part of a (schematic) Busse balloon for slowly changing parameters. Schematic depiction of a path that a spatially periodic pattern may follow during decreasing precipitation, after it crosses the boundary of the Busse balloon.

of decreasing a cannot work if the left boundary $k_l(a)$ of the Busse balloon is not an increasing function of a . It is remarkable that all Busse balloons constructed in this work have a boundary $k_l(a)$ that is an increasing function of a up to the point where k achieves its maximal value. Now, since the left boundary of the Busse balloons for the GKGS-system have this specific shape (see Figure 5.1), the internal dynamics will force the pattern to decrease its wavenumber a little and cross the boundary of the Busse balloon for this smaller wavenumber, so that a new (stable) spatially periodic pattern with a smaller wavenumber appears. This is confirmed by numerical simulations [87].

See Figure 5.1. Homoclinic patterns come as limit cases for spatially periodic patterns for small wavenumbers (homoclinic patterns have wavenumber $\kappa = 0$). From the Busse balloons in Figure 5.1 one deduces that also for the GKGS-system (1.1) in realistic parameters, the homoclinic pattern is the last pattern destabilizing for decreasing a . This once more confirms Ni's conjecture [60] that has been discussed in chapter 5. Therefore, we conclude that 'oasis'-like patterns, i.e. small patches of vegetation without any other vegetation in a large area surrounding, are the last remaining vegetated patterns and can no longer adapt to any other pattern at the rim of desertification.² On the other hand, it is in principle possible that oasis-like patterns are *not* at the edge of desertification, as there exists a range $(a_0^-(\nu), a_0^+(\nu))$ of precipitation rates for which homoclinic patterns exist. Since homoclinic patterns are stable for each $a \in (a_0^-(\nu), a_0^+(\nu))$, oasis-like patterns appear naturally in realistic settings (although we are aware that there are many other mechanisms that may explain the appearance of oasis states – such as the existence of a local water well).

²See also the discussion in §5.3.

5.3 Future work

The Busse balloons depicted in Figure 5.1 give a complete overview of the stable spatially periodic patterns described by the GKGS-model (1.1). By depicting all wavenumbers for all possible choices of a system parameter, they are in fact a graphically displayed parametrization of all stable spatially periodic patterns that solve the system under study. Their boundaries are associated to destabilization mechanisms of the (stable) spatially periodic patterns. By a (numerical) scrutiny of the spectrum associated to the linearization of a solution at the boundary of the Busse balloon, one generally specifies the type of instability that the pattern undergoes when it crosses the boundary.

One crucial assumption made throughout this thesis is that all other³ parameters of the system are constant in time. In reality, of course, this is never the case. For example, the evaporation rate L in (1.1) depends on temperature, humidity and other environmental factors that are not constant in time, even not when one averages over longer periods of time, and therefore L itself is not constant in time.

As indicated in section 5.2.0.1, when a pattern with some fixed wavenumber reaches the boundary of the Busse balloon while the precipitation rate a is slowly decreasing, it will change to a stable pattern with a smaller wavenumber. Exactly *how* this happens is not completely clear and needs further analysis.

If the precipitation rate L decreases even further, and the wavenumber of the pattern has been adapted several times, the pattern gradually approaches the axis $\kappa = 0$. Future research should at least in part focus on the specific characteristics of the dynamics at the boundary of the Busse balloon that lead to desertification. This way, one may be able to deduce early warning signals if desertification is imminent.

An other very relevant question arises when we add a second spatial coordinate y to the model. Notice Klausmeier's original model naturally incorporates two spatial coordinates x and y . In the GKGS-model with two spatial coordinates, a more realistic description of vegetation patterns can be given. Two-dimensional spotted patterns, striped patterns and other coherent structures may then be described, as well as their instabilities.

³That is, all parameters different from the one used to construct the Busse balloon.